

## Seismic performance and damage assessment of reinforced concrete bridge piers with lap-spliced longitudinal steels

Young S. Chung<sup>†</sup>, Chang K. Park<sup>‡</sup> and Eun H. Lee<sup>‡†</sup>

*Department of Civil Engineering, Chung-Ang University,  
San 40-1, Naeri, Daedeogmyeon, Anseong Gyeonggi-Do, 456-756, Republic of Korea*

*(Received June 9, 2003, Accepted October 11, 2003)*

**Abstract.** It is known that lap splices in the longitudinal reinforcement of reinforced concrete (RC) bridge columns are not desirable for seismic performance, but it is sometimes unavoidable. Lap splices were practically located in the potential plastic hinge region of most bridge columns that were constructed before the 1992 seismic design provisions of the Korea Bridge Design Specification. The objective of this research is to evaluate the seismic performance of reinforced concrete (RC) bridge piers with lap splicing of longitudinal reinforcement in the plastic hinge region, to develop an enhancement scheme for their seismic capacity by retrofitting with glassfiber sheets, and to assess a damage of bridge columns subjected to seismic loadings for the development of rational seismic design provisions in low or moderate seismicity region. Nine (9) test specimens with an aspect ratio of 4 were made with three confinement ratios and three types of lap splice. Quasi-static tests were conducted in a displacement-controlled way under three different axial loads. A significant reduction of displacement ductility was observed for test columns with lap splices of longitudinal reinforcements, whose displacement ductility could be greatly improved by externally wrapping with glassfiber sheets in the plastic hinge region. A damage of the limited ductile specimen was assessed to be relatively small.

**Key words:** RC bridge pier; seismic performance; lap splice; retrofit; glassfiber; quasi-static test.

---

### 1. Introduction

Even though earthquakes have economic, social, psychological, and even political effects in regions or the countries where they take place, Korea is considered to be immune from the earthquake hazards since it is located rather far away from the active fault area. However, it has been observed in the Korean Peninsula that the number of minor or low earthquake motions have increased year by year. The collapse or near collapse of bridge superstructures during the 1994 Northridge earthquake and the 1995 Kobe earthquake also stimulated the evaluation of seismic performance of various infrastructures which were seismically or nonseismically designed in Korea.

---

<sup>†</sup> Professor

<sup>‡</sup> Ph. D Candidate

<sup>‡†</sup> Graduated Student

Lap splices of longitudinal steels were sometimes practically located in the lower plastic hinge region of most RC bridge columns that were constructed before the seismic design code of Korea bridge design specifications (Ref. 6) were implemented in 1992. Therefore, it is needed to investigate the effect of lap splices and retrofit scheme on the lap spliced piers.

By investigating bond action between concrete and deformed bars in lap splices, Tepfers (1982) found that providing confinement reinforcement increased the bond capacity and recommended that the effect of confining reinforcement would be added to the splitting resistance of the concrete. Einea *et al.* (1999) also found that the lateral confinement provided by the transverse reinforcement had a beneficial effect on increasing the compressive strength of confined concrete, and the ductility of the member. A number of researchers (Chai 1991, Priestley 1997, Jaradat 1998, Aboutaha 1999, Chung 1999, and Chang 2000) have investigated the effect of confinement and retrofit on piers. Consequently, it has been well known that one of the most economical retrofit strategies for aged bridge piers is to provide transverse confinement. They found that transverse confinement in the plastic hinge region was effective in enhancing the flexural strength and ductility capacity of the column. The onset of strength degradation was delayed due to the longer splice length. Priestley (1997) indicated that the confinement reinforcement, not the lap length, was the key factor for the prevention of splice failure in the columns when the lap length was longer than  $20d_b$ . Jaradat *et al.* (1998) showed from test results of columns with steel jackets that while test columns with inadequate lap splices experienced very dramatic splice failure, the retrofitted column exhibited improved displacement ductility up to a displacement ductility factor of 6. Chung *et al.* (1999) showed the effect of glassfiber sheets for the seismic enhancement of RC bridge piers through the quasi-static cyclic load test. Chang *et al.* (2000) investigated the influence of lap splice of longitudinal bars in the plastic hinge zone on the nonlinear behavior characteristics of RC piers through the scale model tests, and proposed new seismic detailing concept appropriate to moderate seismicity region.

In this research, the effect of lap splice, axial force, retrofit, and transverse confinement was investigated. Nine(9) test specimens with an aspect ratio of 4.0 were made with three confinement ratios and two types of lap splice. Transverse confinement was provided by steel reinforcement and the retrofit material like fiber jacket. To provide different levels of transverse confinements as shown in Table 2, test specimens can be categorized into three groups which were designed in accordance with the pre-1992 design code, the 1992 seismic design code, and the limited ductility design concept. Since longitudinal lap splices of bridge piers are sometimes practically unavoidable, three test specimens including two retrofit specimens were made with lap splices for half (50%) longitudinal reinforcement steels, and another specimen was done with lap splices in all (100%) longitudinal reinforcing steels. Three alike nonseismic specimens were included so that the effect of axial load was investigated. In addition, two more specimens were provided in accordance with the limited ductile design and the 1992 seismic design concept. The objective of these quasi-static tests is to evaluate the seismic performance of RC bridge piers with lap splicing of longitudinal reinforcement in the plastic hinge region, to investigate the enhancement of their seismic capacity by retrofitting with glassfiber sheets, and to evaluate a damage of bridge piers subjected to seismic loadings for the development of appropriate transverse confinement ratios for bridge columns in low or moderate seismicity regions, like Korea.

## 2. Material properties

10 mm-diameter deformed steel was used as the longitudinal steel in the RC test specimens, of which confinement steels had been laterally used with 6 mm-diameter deformed steel. The yield stress from tensile coupon testing was 450.8 MPa for  $\phi 10$  deformed steel and 352.8 MPa for  $\phi 6$  deformed steel. The area ratio of longitudinal reinforcement steels was considered as  $\rho = 1.13\%$ . The target compressive strength of concrete was  $f'_c = 23.52$  MPa.

Two nonseismic test specimens with 50% lap splicing were wrapped with one layer of glassfiber sheet around their potential plastic hinge region, of which physical properties are shown in Table 1. The thickness of the glassfiber sheet was computed using Eq. (1) of Priestley *et al.* (1996).

$$t_j = \frac{0.1(\varepsilon_{cu} - 0.004)Df'_{cc}}{f_{uj}\varepsilon_{uj}} \quad (1)$$

where  $t_j$  is the thickness of glassfiber sheet,  $\varepsilon_{cu}$  and  $\varepsilon_{uj}$  are the ultimate strain of confined concrete and glassfiber sheet, respectively.  $D$  is the diameter of test specimen,  $f'_{cc}$  is the stress of confined concrete at peak, and  $f_{uj}$  is the ultimate stress of glassfiber sheets.

Table 1 Physical properties of glassfiber sheets

Classification	Tensile Strength (MPa)	Tensile modulus (MPa)	Elongation (%)	Thickness (mm)
TYFO SEH 51	550	24,700	2.0	1.3
CAF GL-1000	490	24,500	2.3	1.0

## 3. Test program

### 3.1 Test specimens

A circular solid RC piers now in service was adopted as a prototype of this test. The bridge had been designed in accordance with the 1992 seismic design provisions of Korea bridge Design Specification (Ref. 6). Fig. 1 shows detailed dimensions of all test columns. As shown in Table 2, nine test specimens were prepared for the quasi-static test to investigate their seismic performance. Seven test columns were nonseismically designed on the basis of the pre-1992 design code. Among them, three specimens (N-SP00-P1,2,3-R0) were made without lap splice of the longitudinal reinforcement steel, three specimens (N-SP05-P1-R0,1,2) were made with lap splice of 50% longitudinal reinforcement steels, and another specimen (N-SP10-P1-R0) was made with lap splice of 100% longitudinal reinforcement steels. The lap length of longitudinal reinforcement steels was computed as  $28d_b$  for D10 compressive bars, where  $d_b$  is are the diameter of the bar. The other two specimens (N,L-SP00-P1-R0) were designed in accordance with the 1992 seismic design code of Korea bridge design specifications, and with the limited ductile design concept, as shown in Table 2.

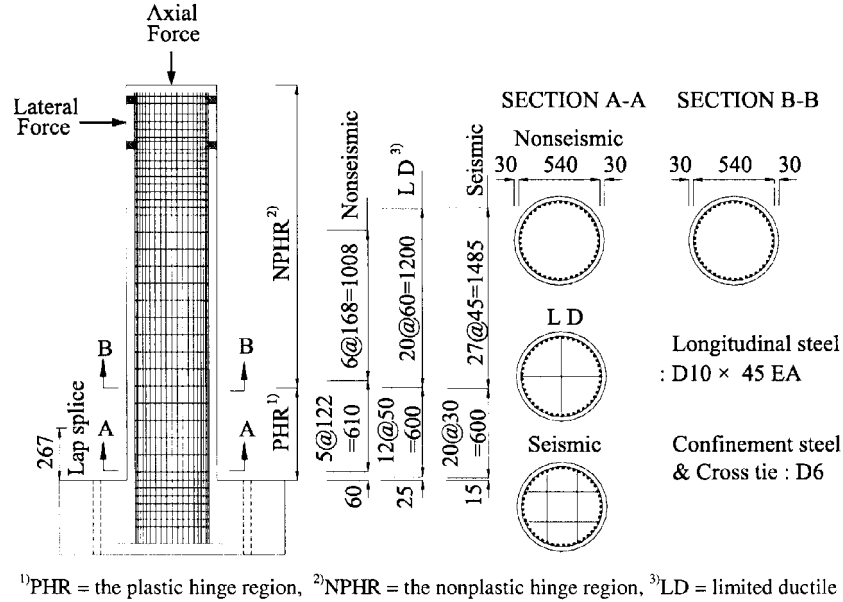


Fig. 1 Details of test specimens (Unit : mm)

Table 2 Characteristics of test specimens

Design Concept	Nomenclature *	Number of Longitudinal spliced bars	Number of Cross Tie at PHR ** (EA)	Space of Transverse steel PHR/NPHR ** (mm.)	Axial Force $P = \alpha f'_c A_g$ (KN)	Retrofit Glass fiber	
Non seismic	N-SP00-P1-R0	None (0%)	None	122/168	664.4 ( $\alpha = 0.1$ )	None	
	N-SP00-P2-R0				1,330 ( $\alpha = 0.15$ )		
	N-SP00-P3-R0				1995 ( $\alpha = 0.2$ )		
	N-SP05-P1-R0	Half (50%)			664.4 ( $\alpha = 0.1$ )		SEH-51
	N-SP05-P1-R1				CAFGL1000		
	N-SP05-P1-R2						
	N-SP10-P1-R0	All (100%)					
Limited Ductile	L-SP00-P1-R0	None (0%)	2	5/6			
Seismic	S-SP00-P1-R0		4	3/4.5			

\*N = Nonseismic ; L = Limit Ductile ; S = Seismic ; SP = Splicing ; P = Axial Force ; R = Retrofit

\*\*See Fig. 1 for PHR/NPHR

### 3.2 Cyclic loads

Quasi-static tests were carried out in a displacement-controlled way. Cyclic loads were applied at the top of test columns using 1,000 KN hydraulic actuator, as shown in Photo 1. As shown in

Fig. 2(a), the yield displacement,  $\Delta_y$  was, in a load control mode, computed as  $\frac{\epsilon_{sy}}{\epsilon_{mea}} \Delta_{mea}$ , where

$\epsilon_{sy} = 0.002$  denotes the yield strain of the longitudinal steel.  $\epsilon_{mea}$  and  $\Delta_{mea}$  denote the measured strain of the longitudinal steel and the measured lateral displacement of the column, respectively, which were corresponding to the 75% theoretical yield load,  $F_y$ . Fig. 2(b) shows the cyclic displacement ductilities, which were the magnitude of applied lateral displacement to the yield displacement. Three levels of axial load,  $0.1f'_c A_g$ ,  $0.15f'_c A_g$ , and  $0.2f'_c A_g$ , were applied to investigate the effect of axial load on the seismic performance.

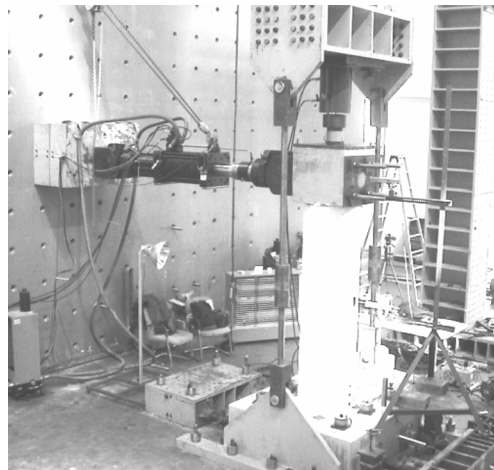
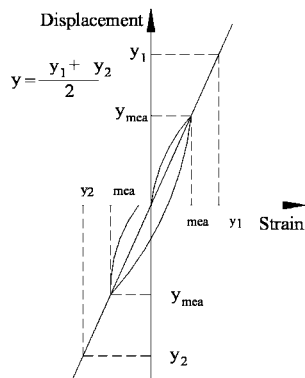
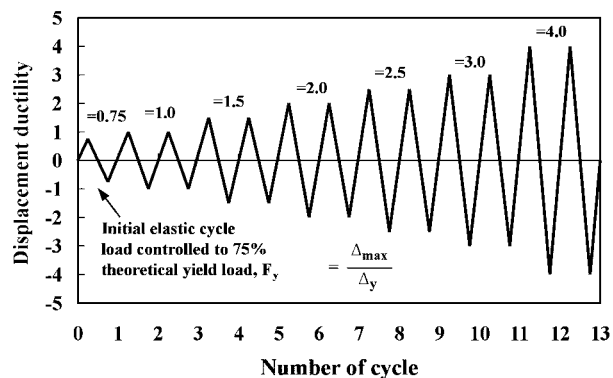


Photo 1 Test setup



(a) Yield displacement



(b) Load cycles

Fig. 2 Cyclic load pattern

## 4. Test results and discussions

### 4.1 Lateral force-displacement behavior

Lateral force displacement hysteresis loops for all test columns are shown in Fig. 3. Figs. 3(a), 3(b), and 3(c) show that test specimen (N-SP00-P1-R0) without lap splices developed more stable hysteresis loops than two test specimens (N-SP05,SP10-P1-R0) with lap splice of longitudinal steels. It was also observed from Figs. 3(a), 3(f), and 3(i) that the increase of axial force induced a slight reduction of the displacement ductility. As shown in Figs. 3(b), 3(e), and 3(h), it was found that the glassfiber sheets remarkably increased the displacement ductility. In addition, Figs. 3(a), 3(d), and 3(g) showed that test specimens with more transverse reinforcement could give bigger displacement ductility. Fig. 4 shows comparative lateral force displacement envelope curves which were discussed about four test parameters: the transverse confinement, lap splice, axial force, and retrofit. Fig. 4(a) shows that more transverse confinement in the plastic hinge region of RC bridge columns increases the ultimate deformation. It is also observed that a significant reduction of the displacement ductility ratio was observed in test specimens with lap splices of longitudinal steel

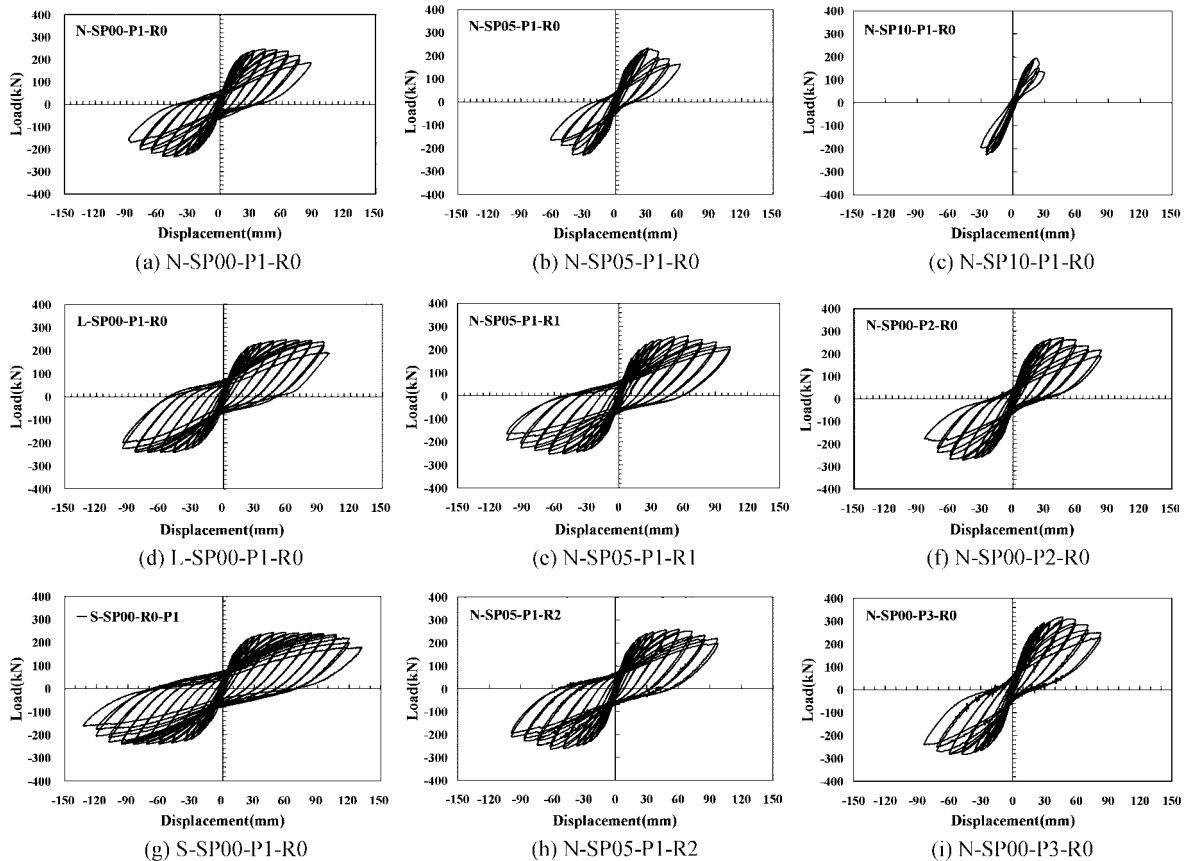


Fig. 3 Lateral force-displacement hysteresis loops

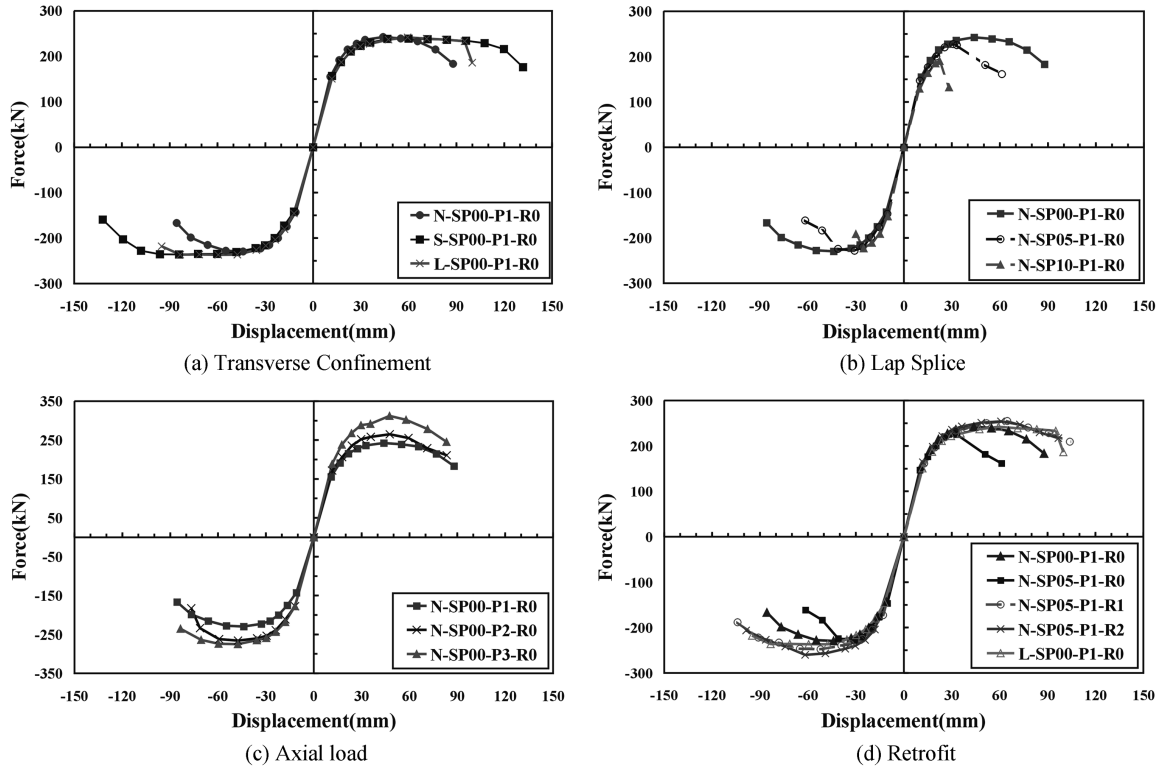


Fig. 4 Lateral force-displacement envelope curve

from Fig. 4(b). Fig. 4(c) shows that the axial force increases the lateral resisting force. Fig. 4(d) shows that in spite of the lap splicing, the displacement ductility of retrofitted specimens (N-SP05-P1-R1, R2) were bigger than that of the reference specimen (N-SP00-P1-R0), and equivalent to that of the limited ductile specimen (L-SP00-P1-R0).

#### 4.2 Displacement and strain energy ductility

Displacement ductility is one of the key factors for the evaluation of the seismic performance of RC bridge piers. The yield displacement,  $\Delta_y$ , was explained in Fig. 2(a). The ultimate displacement was defined as the lesser of the measured displacements between when longitudinal or confinement steel exceed its fracture state, and when the strength on the descending branch of the force-displacement envelope curve becomes less than  $0.85V_{max}$ . The displacement ductilities for the test specimens,  $\mu_\Delta = \Delta_u/\Delta_y$  are shown in Table 3. It can be observed that the use of glassfiber sheets for test specimen (N-SP05-P1-R1,2) increased the displacement ductility ratio by above 67% with respect to the displacement ductility factor of the corresponding reference test specimen (N-SP05-P1-R0). The displacement ductility ratio of 100% lap spliced test specimen (N-SP10-P1-R0) was significantly reduced to approximately 36% of those for non-spliced test specimen (N-SP00-P1-R0).

Strain energy ductilities,  $\mu_E = E_u/E_y$ , are computed and shown in Table 3. As shown in Fig. 5, the areas  $\Delta OAC$  and  $\square OABD$  are the yield strain energy prior to the specimen yielding,  $E_y$ , and the ultimate strain energy when the specimen reached the ultimate state,  $E_u$ , respectively. The energy ductilities of all test specimens showed similar trends to the displacement ductility on test parameters : lap splice of longitudinal steel, axial force, transverse confinement, and retrofit. Significant reduction of strain energy ductility ratio was observed for test specimens (N-SP05,10-P1-R0) with the lap splice of longitudinal steels in the plastic hinge region, comparing to the strain energy ductility ratio of the corresponding nonspliced test specimen (N-SP00-P1-R0). The use of glassfiber sheets increased the strain energy ductility of the nonseismic specimens with lap splice of 50% longitudinal reinforcement steels as high as that of the limited ductility specimen. This means that the retrofit scheme, when effectively used, can improve the seismic performance of existing bridge piers so that the use of fiber jackets can become an appropriate retrofit measure in low and moderate seismicity zones.

Table 3 Experimental ductility ratio

Specimen	Displacement				Strain Energy			
	Yield (mm)	Ultimate (mm)	Ductility	Normalized*	Yield (kN · mm)	Ultimate (kN · mm)	Ductility	Normalized*
N-SP00-P1-R0	10.8	79.8	7.4	1.00	996	16400	16.5	1.00
N-SP00-P2-R0	11.8	73.8	6.3	0.85	1193	16190	13.6	0.82
N-SP00-P3-R0	11.7	75.9	6.5	0.88	1355	19450	14.4	0.87
N-SP05-P1-R0	10.1	46.9	4.6	0.62	898	10790	12.0	0.73
N-SP05-P1-R1	12.7	98.8	7.8	1.05	1230	20960	17.0	1.03
N-SP05-P1-R2	11.9	94.8	8.0	1.08	1194	20530	17.2	1.04
N-SP10-P1-R0	9.8	25.8	2.6	0.35	713	3390	4.8	0.29
L-SP00-P1-R0	11.7	97.9	8.4	1.14	1102	20690	18.8	1.14
S-SP00-P1-R0	11.9	123.7	10.4	1.41	1159	26350	22.7	1.38

\*Normalized ductilities were computed with respect to the ductility of the reference specimen, N-SP00-P1-R0.

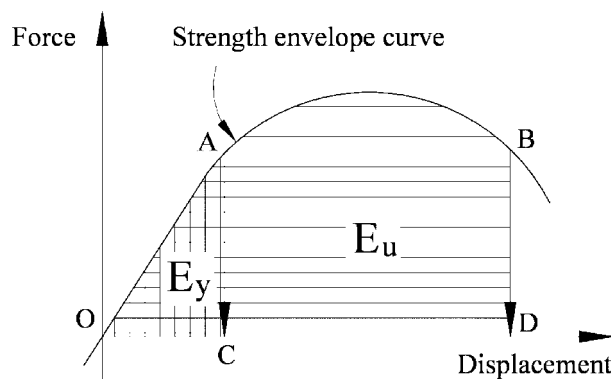


Fig. 5 Definition of the yield and ultimate strain energy

### 4.3 Energy absorption capacity

Fig. 6 shows the comparative curves of the cumulative energy absorption capacity of all test specimens on four test parameters. The amount of absorption energy in each load cycle has been calculated from the hysteresis loop between two consecutive displacement peaks. As shown in Fig. 6(a), the limited ductile test specimen (L-SP00-P1-R0) and seismic test specimen (S-SP00-P1-R0) showed more energy absorption capacity by about 65% and 71%, respectively, as compared to the nonseismic test specimen (N-SP00-P1-R0) without lap splice. It was also found from Fig. 6(b) that the energy absorption capacity of test specimen (N-SP05-P1-R0) with lap splice of 50% longitudinal reinforcement steels decreased by about 63% as compared to the energy absorption capacity of the nonspliced test specimen (N-SP00-P1-R0). It is seen from Fig. 6(c) that the increase of axial load slightly increased the energy absorption capacity. Fig. 6(d) shows that the retrofitted specimens (N-SP05-P1-R1,2) with glassfiber sheets increased the energy absorption capacity by above 92% as compared to the non-retrofitted test specimen (N-SP05-P1-R0), of which the energy absorption capacity was only 63.2% of the reference specimen, N-SP00-P1-R0.

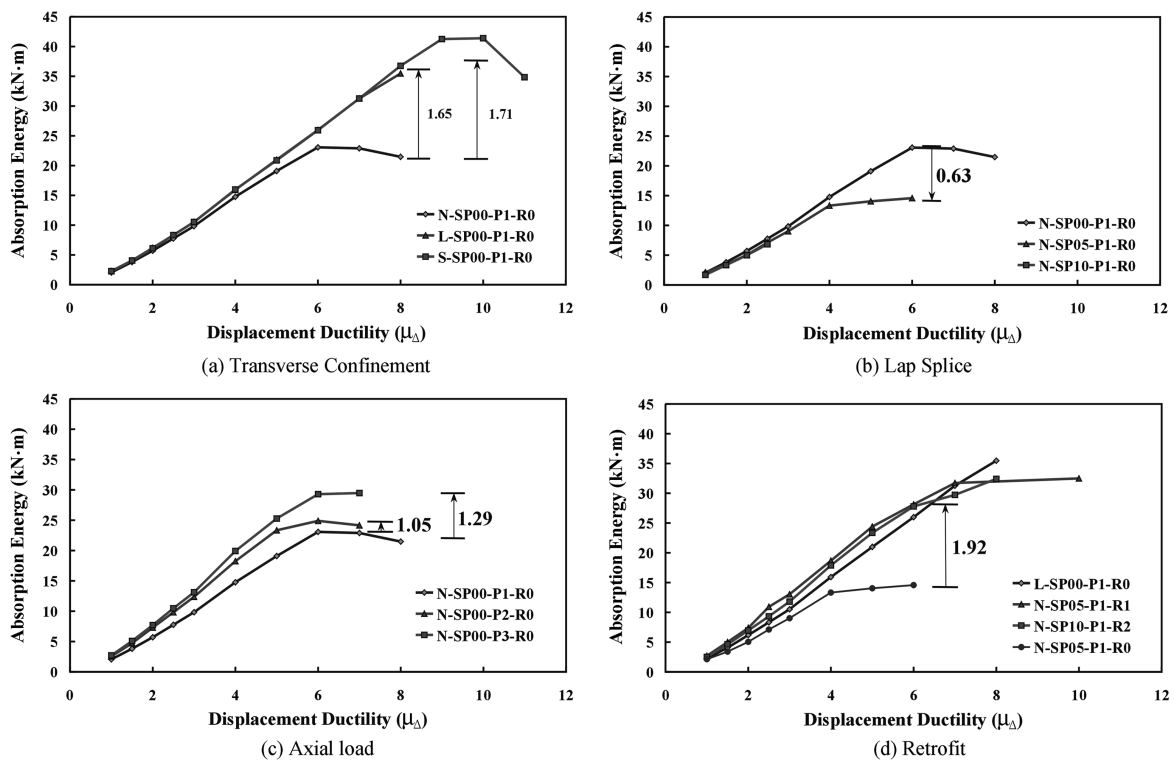


Fig. 6 Comparative energy absorption capacity

### 4.4 Strength degradation

Strength degradation of test columns can be obtained by normalizing the lateral applied loads with respect to the lateral yield load as shown in Fig. 7. The steeper descending slope in the figure

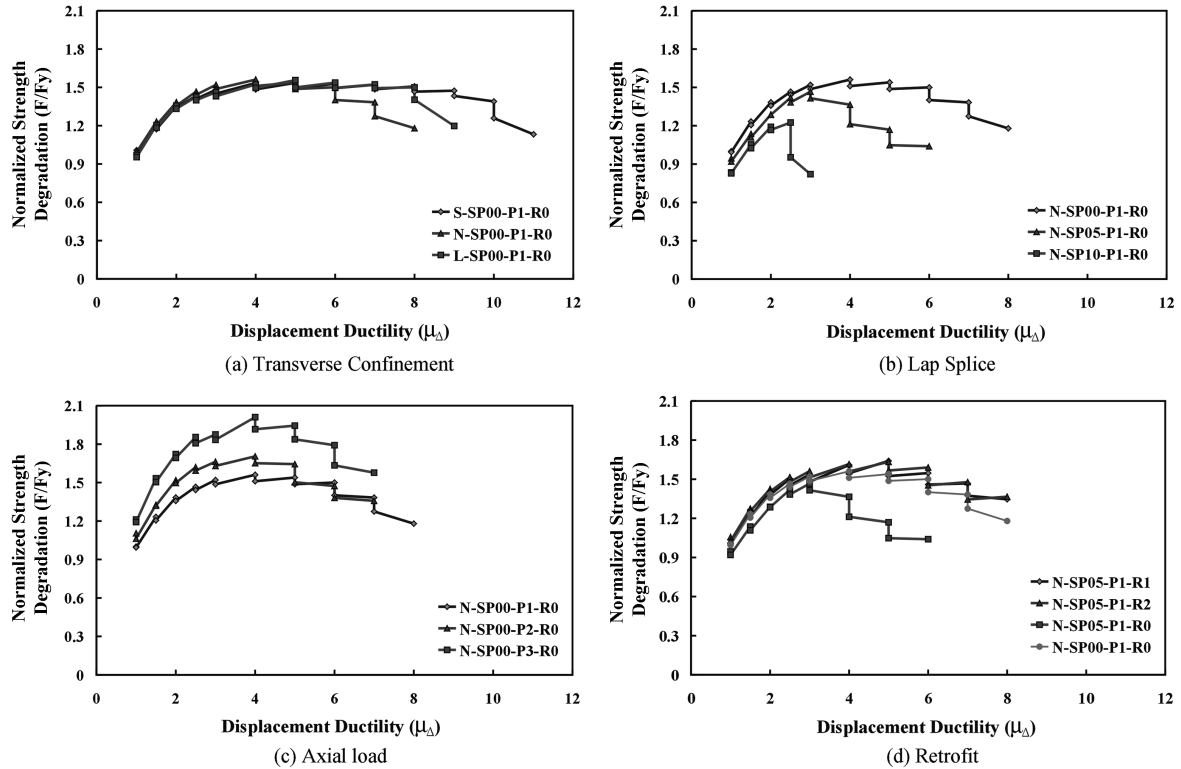


Fig. 7 Normalized strength degradation

implies a larger strength drop. It is clearly shown from Fig. 7(a) that specimens designed according to the seismic design code and the limited ductility design concept had flatter curves compared to the nonseismic specimens. As shown in Fig. 7(b), specimens with lap splices showed significant strength loss compared to specimens without lap splices. Fig. 7(c) shows that the specimen under higher axial force had bigger lateral strength, but showed more excessive strength drop at larger deformation levels. It is seen in Fig. 7(d) that the use of glassfiber sheets remarkably decreased the magnitude of the strength drop.

#### 4.5 Strain of transverse reinforcing steels

Because the lack of adequate lateral reinforcement results in premature yielding of transverse reinforcement and rapid deterioration of the pier, strains measured from the transverse reinforcement can be one of the factors that can be used to evaluate the seismic performance. Strains measured from the transverse reinforcement at the center of the plastic hinge zone are shown in Fig. 8. Figs. 8(a), 8(b), and 8(d) show the strain of transverse steels in the lap-spliced specimens and in the retrofit specimen below 1000 microstrain, respectively. This implies that the retrofit specimen was laterally well confined, so that the transverse lateral reinforcement of retrofit specimen experienced higher strain than that of lap-spliced specimens until failure. In Fig. 8(c), the transverse steel even in non-spliced specimen was below the yield strain until the specimen failed. It is shown

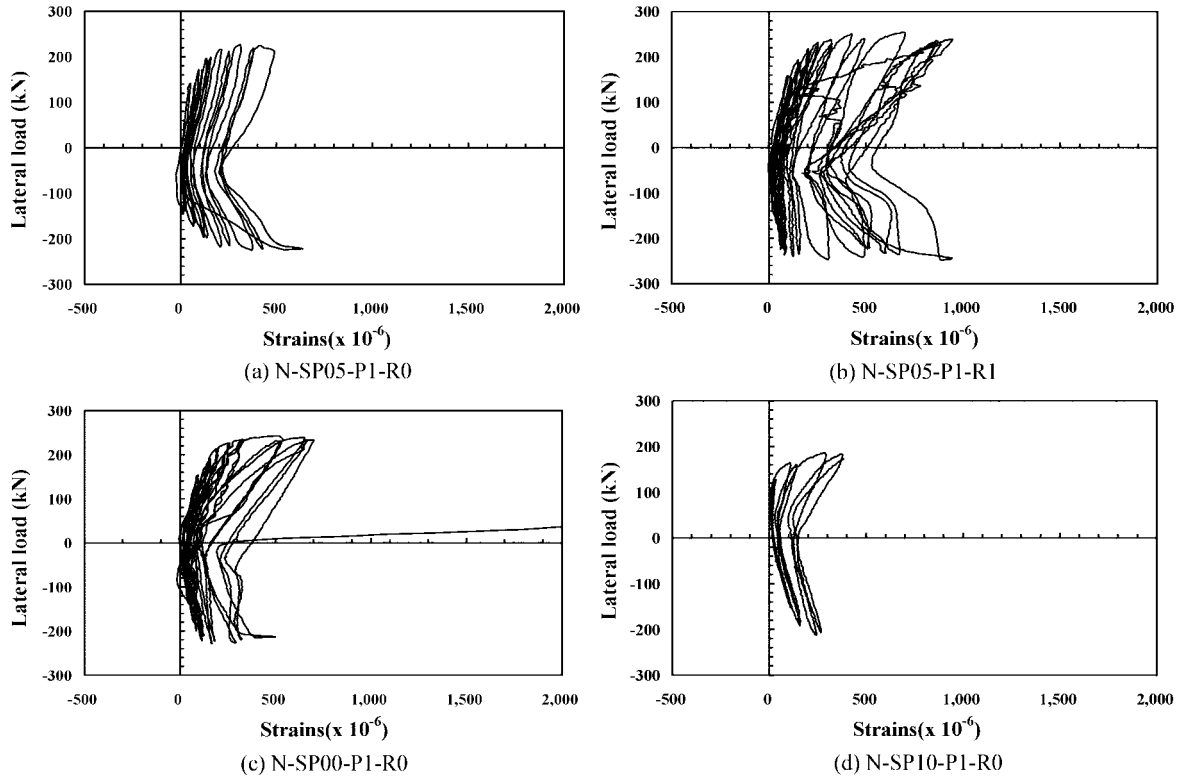


Fig. 8 Strain of transverse reinforcing steels

from Figs. 8(a) and 8(d) for lap-spliced specimens that the specimens failed at very low strain of the transverse steel because of the slip of the longitudinal reinforcement at the failure of the specimen.

## 5. Damage assessment

Based on the experience from previous earthquakes and laboratory investigations, damage of reinforced concrete structures is the result of a combination of the maximum deformation and the effect of repeated cyclic loading, a phenomenon generally known as low-cycle fatigue. Thus, a ductility ratio as a sole measure of damage is not sufficient as a damage indicator for our purposes. The number of cycle, or rather the dissipated energy has to be taken into account as well.

Of the more recent damage models, the model of Park and Ang (1985) was used for this research,

$$D = \frac{\delta_M}{\delta_u} + \frac{\beta}{Q_y \delta_u} \int dE \quad (2)$$

where,  $\delta_M$  = maximum deformation experienced so far;  $\delta_u$  = ultimate deformation under monotonic loading;  $Q_y$  = calculated yield strength;  $dE$  = dissipated energy increment; and  $\beta$  = coefficient of cyclic loading effect.

The damage of test columns was computed based on the Park and Ang Model, and plotted in Fig. 9. The  $\beta$  value of Eq. (2) was inversely calculated by assuming the damage indices  $D = 1.0$  when the ultimate displacement in 4.2 was attained at failure. Table 4 shows the resulting  $\beta$  value for all specimens. Fig. 9 shows progressive damage indices with increasing displacement ductility, which were analyzed on four test parameters: transverse confinement, lap-splice, axial force, and fiber retrofit. As shown in Fig. 9(a), it was observed bigger damage on the specimen with less transverse confinement, comparing with other two specimens L-SP00-P1-R0 and S-SP00-P1-R0. Initial cracks were occurred at approximate 2~3 displacement ductilities, which induced 0.2 for the damage index. Fig. 9(b) shows comparative damage indices reflecting the effect of the lap-splice of longitudinal reinforcing steels. Similarly, rapid increase of damage was observed for the lap-spliced specimens. The 100% lap-spliced specimen, N-SP10-P1-R0, showed initial cracks at 1.0 displacement ductility and failed due to the slip of lap-spliced steels. Fig. 9(c) shows the damage level on three levels of axial force. There were observed some effect of axial force on the seismic damage, which seemed to be insignificant. Fig. 9(d) shows the comparative damage indices for the reference lap-spliced specimen, two retrofit specimens with glassfiber sheet, the limited ductile specimen, and the seismic specimen. It could be confirmed the effectiveness of fiber retrofit that even in spite of the lap splice, the seismic performance of retrofitted specimens could reach to that of the limited ductile specimen, L-SP00-P1-R0.

Since all the specimens of this research were designed with a strong footing, most of cracking

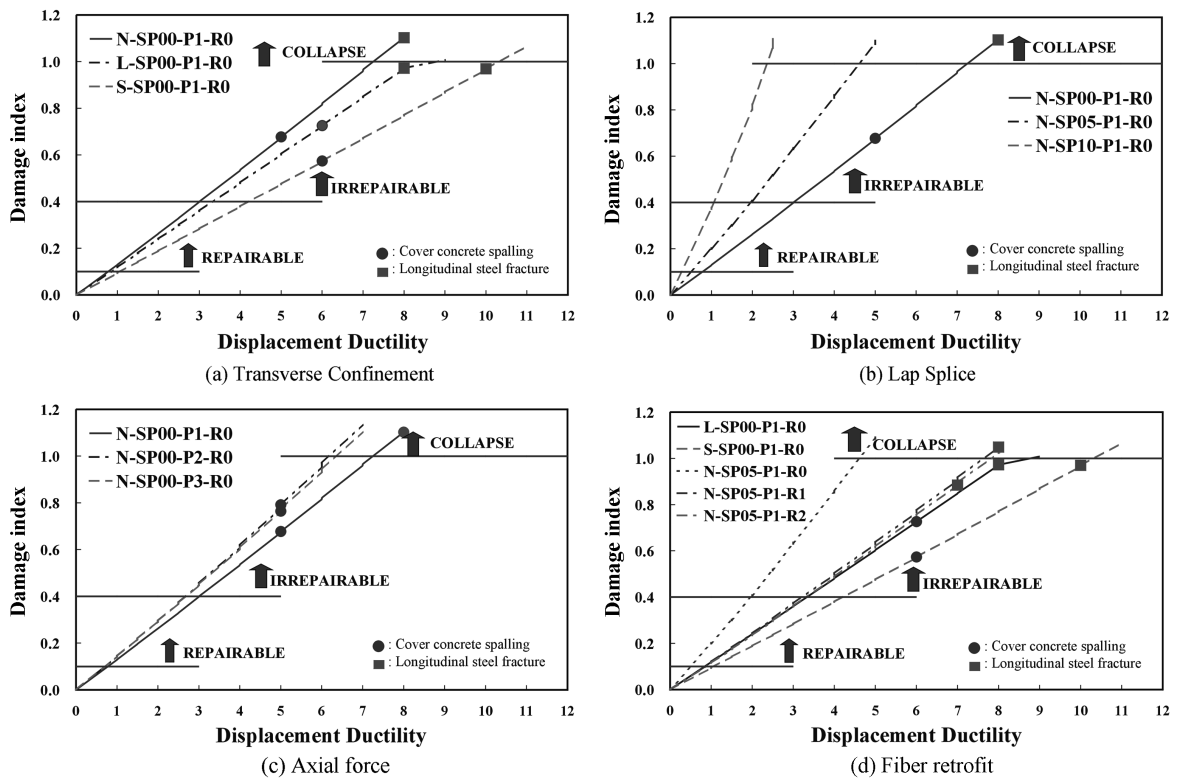


Fig. 9 Damage assessment

damages were concentrated within the plastic hinge region in flexural failure mode. The specimens without lap-splice failed due to bond failure and buckling of the longitudinal reinforcement, but the specimen with lap-spliced failed due to the slip of the lap-spliced steels. The longitudinal reinforcing bars initially fractured at the displacement ductility,  $\mu = 7\sim 8$ . These damage indices were compared with the actual damage state of specimens experienced during the quasi-static test, as shown in Table 4. Table 4 shows the sequential damage state that were visually observed in the plastic hinge zone, and damage indices which were computed with increasing displacement ductility by the Park and Ang model, Eq. (2). For retrofitted specimens, concrete cracks could not be visually observed because of glassfiber sheet, but at the displacement ductility level of  $\mu = 3.0$ , crack were occurred at cold joint between column and footing. Rebar fractures were not observed at two lap-spliced specimens, N-SP05-P1-R0 and N-SP10-P1-R0, which were failed due to the slip of the lap-spliced longitudinal steels.

Table 4 Damage assessment at displacement ductility

Specimen	Ductility ( $\mu$ )											$\beta$ of Eq. (2)				
	1.0	1.5	2	2.5	3	4	5	6	7	8	9		10	11		
N-SP00-P1-R0	0.129	0.196	0.262	0.329	0.398	0.533	0.673	0.816	0.959	1.000						0.0066
N-SP00-P2-R0	0.143	0.217	0.293	0.370	0.450	0.609	0.778	0.955	1.000							0.0181
N-SP00-P3-R0	0.144	0.217	0.293	0.369	0.447	0.603	0.765	0.933	1.000							0.0135
N-SP05-P1-R0	0.200	0.299	0.406	0.516	0.630	0.852	1.000									0.0172
N-SP05-P1-R1	0.118	0.181	0.243	0.306	0.376	0.498	0.630	0.767	0.906	1.000						0.0107
N-SP05-P1-R2	0.115	0.174	0.235	0.296	0.359	0.485	0.614	0.747	0.885	1.000						0.0113
N-SP10-P1-R0	0.372	0.581	0.801	1.000												0.0956
L-SP00-P1-R0	0.118	0.178	0.240	0.299	0.360	0.479	0.601	0.725	0.848	0.970	1.000					0.0011
S-SP00-P1-R0	0.094	0.141	0.189	0.235	0.283	0.379	0.474	0.571	0.670	0.768	0.867	1.000	0.966			0.0019

♣ rebar buckling      ● cover concrete spalling      ■ rebar fracture  
 ♠ crack at cold joint between footing and column

## 6. Conclusions

The following conclusions can be made

- Nonseismic RC bridge piers, with lap splice of longitudinal reinforcement in the plastic hinge region, appeared to fail at low ductility level. This was due to the slip of the lap-spliced steels, which resulted from the insufficient development length or confining stress. Accordingly, it is

desirable to prohibit the lap splice of longitudinal steels within the potential plastic hinge region even in low or moderate seismicity regions.

- b) Even limited ductility design specimen showed considerably larger displacement ductility capacity which could be enough for in low or moderate seismic region. Appropriate modification should be needed in the current seismic provisions for the lateral confinement of bridge columns.
- c) Two test columns (N-SP05-P1-R1,2) externally wrapped with glassfiber sheets showed a significant improvement of displacement ductility, even in spite of the lap splice in the plastic hinge region.
- d) Taking into consideration of nonlinear behavior characteristic and damage indices for the limited ductile specimen, seismic requirement in moderate seismicity region must be reviewed in detail.

## Acknowledgements

The author gratefully acknowledge the support from the Korea Earthquake Engineering Research Center(Contract No. 2000G0302). The author also thank Conclnic Co. for providing experimental specimens.

## References

- Aboutaha, R.S., Engelhardt, M.D., Jirsa, J.O. and Kreger, M.E. (1999), "Experimental investigation of seismic repair of lap splice failures in damaged concrete columns", *ACI Struct. J.*, **96**(2), 297-307.
- Chang, S.P., Kim, J.K., Kim, I.H. and Lim, H.W. (2000), "The influence of lap splice of longitudinal bars in the plastic hinge zone on the nonlinear behavior characteristics of RC piers and new seismic detailing concept in moderate seismicity region", *Proc. the Earthq. Eng. Soc. Korea Conf.*, **4**(1), 335-340.
- Chai, Y., Priestley, M.J.N. and Seible, F. (1991), "Seismic retrofit of circular bridge columns for enhanced flexural performance", *ACI Struct. J.*, **88**(5), 572-584.
- Chung, Y.S., Lee, K.K., Han, G.H. and Lee, D.H. (1999), "Quasi-static test for seismic performance of circular R.C. bridge piers before and after retrofiting", *J. of the Korea Concrete Institute*, **11**(5), 107-118.
- Einea, A., Yehia, S. and Tadros, M.K. (1999), "Lap splices in confined concrete", *ACI Struct. J.*, **96**(6), 947-955.
- Jaradat, O.A., McLean, D.I. and Marsh, M.L. (1998), "Performance of existing bridge columns under cyclic loading - Part 1: Experimental results and observed behavior", *ACI Struct. J.*, **95**(6), 695-704.
- Ministry of Construction and Transportation (2000), "Korea highway bridge design specification", Korea Road & Transportation Association.
- Park, Y.J. and Ang, Alfredo H.-S. (1985), "Mechanistic seismic damage model for reinforced concrete", *J. of Struct. Eng.*, **111**(4), APR., 722-739.
- Priestley, M.J.N., Seible, F. and Calvi, G.M. (1996), *Seismic Design and Retrofit of Bridges*, John Wiley & Sons Inc., New York.
- Priestley, M.J.N., Seible, F., MacRae, G.A. and Chai, Y. (1997), "Seismic assessment of the Santa Monica Viaduct Bent details", *ACI Struct. J.*, **94**(5), 513-524.
- Saadatmanesh, H., Ehsani, M.R. and Jin, L. (1996), "Seismic strengthening of circular bridge pier models with fiber composites", *ACI Struct. J.*, **93**(6), 639-647.
- Tepfers, R. (1982), "Lapped tensile reinforcement splices", *ASCE*, **108**, No. ST1, Jan.